J Korean Med Sci. 2023 Nov 27;38(46):e392
https://doi.org/10.3346/jkms.2023.38.e392
eISSN 1598-6357·pISSN 1011-8934

JKMS

Original Article
Basic Medical Sciences

Lymph Node Stations of Pancreas Which Are Identified in Real Color Sectioned Images of a Cadaver With Pancreatic Cancer

Chung Yoh Kim, Yongwook Jung, and Jin Seo Park

Department of Anatomy, Dongguk University School of Medicine, Gyeongju, Korea

Received: Jul 3, 2023
Accepted: Aug 23, 2023
Published online: Nov 15, 2023

Address for Correspondence:
Jin Seo Park, PhD
Department of Anatomy, Dongguk University School of Medicine, 87 Dongdae-ro, Gyeongju 38066, Republic of Korea.
Email: park93@dongguk.ac.kr

ORCID iDs
Chung Yoh Kim
https://orcid.org/0000-0001-8074-076X
Yongwook Jung
https://orcid.org/0000-0002-8482-8694
Jin Seo Park
https://orcid.org/0000-0001-7956-4148

Funding
This work was supported by Anatomage Inc, USA. This research was also supported by a Basic Science Research Program through the National Research Foundation of Korea (NRF) funded by the Ministry Education (NRF-2021R1F1A1063044).

Disclosure
The authors have no potential conflicts of interest to disclose.

ABSTRACT

Background: In pancreatic cancer surgery, anatomical understanding of lymph node metastases is required. Distinguishing lymph nodes in computed tomography or magnetic resonance imaging is challenging for novice doctors and medical students because of their small size and similar color to surrounding tissues. This study aimed to enhance our understanding of the clinical anatomy of lymph node stations relevant to pancreatic cancer using newly sectioned images of a cadaver with true color and high resolution and their three-dimensional (3D) models.
Methods: An 88-year-old female cadaver who died of pancreatic cancer was serially sectioned. Among the sectioned images of the whole body (0.05 mm-sized pixel, 48 bits color), images of the abdomen were selected, and examined to identify lymph nodes and nearby structures. 34 structures (9 in digestive system; 1 in urinary system; 2 in cardiovascular system; 22 in lymphatic system) were segmented on the sectioned images. Based on the sectioned and segmented images, volume and surface models were produced.
Results: Among the known 28 lymph node stations, 21 stations were identified through location, size, and color of normal and abnormal structures in the sectioned images and 3D models. Two near the splenic artery could not be separated from the cancer tissue, and the remaining five were not clearly identified. In the surface models, the shape and location of lymph node stations could be confirmed with nearby structures.
Conclusion: The lymph node stations relevant to pancreatic cancer can be anatomically understood by using the sectioned images and 3D models which contain true color and high resolution.

Keywords: Lymphatic Metastasis; Pancreatic Neoplasms; Cross-Sectional Anatomy; Three-Dimensional Image; Visible Human Projects

INTRODUCTION

Almost all pancreatic cancers are discovered at the terminal stage because there are no specific symptoms. Besides, pancreatic cancer of terminal stage is always accompanied by severe lymph node metastases. To diagnose and resect lymph node metastases early and accurately in pancreatic cancer, anatomy knowledge of the metastases is necessary[1-3]; hence 28 stations of lymph node metastases were presented by the Japan Pancreas Society.[4,5]

Author Contributions

Conceptualization: Kim C, Park JS. Investigation: Kim C, Park JS. Software: Kim C. Supervision: Park JS. Validation: Jung Y. Writing - original draft: Kim C. Writing - review & editing: Park JS.

The 28 lymph node stations were only described on computed tomography images (CT), magnetic resonance images (MRI), and schematic figures.[4,5] However, the lymph node stations were hardly identified in CT and MRI because the lymph nodes were similar in color and CT and MRI were gray color and low resolution. Regarding schematic figures, readers could understand each station intuitively well, but it was challenging to comprehend the stereoscopic location relation of lymph nodes in each station. Therefore, high quality images for the 28 stations were necessary to overcome this inadequacy of CT and MRI, and three-dimensional (3D) models were also required for the stereoscopic anatomy of lymph node stations.

Meanwhile, in 2002, we created sectioned images obtained through serial microsectioning of a young male's entire body via the Visible Korean Project.[6] Subsequently, sectioned images of females and males were created until 2019.[7-11] In the sectioned images, both macro-structures of size < 2,000 mm (e.g., the skin of the whole body) and micro-structures of size of ≥ 0.04 mm (e.g., central retinal vessels[8] and nuclei of cranial nerves in the brainstem[12]) could be identified in real color (24- or 48-bit color). Various two-dimensional (2D) and 3D applications[13-18] and cross sectional anatomy atlases[19,20] have been developed for anatomy and radiology education using these sectioned images. We expected these sectioned images would give us a clear view of pancreatic cancer and its lymph node metastases.

This study aimed to enhance the understanding of the clinical anatomy of lymph node stations relevant to pancreatic cancer through newly acquired sectioned images of a cadaver with real color and high resolution and their 3D models. To achieve this aim, newly sectioned images of the whole body were obtained from a female cadaver with pancreatic cancer, and 3D models from the images were reconstructed. In the sectioned images and 3D models, lymph node stations were identified according to the Japan Pancreas Society Classification.[4,5,21]

METHODS

This study was performed from December 2022 to May 2023 at Ajou University School of Medicine. A female cadaver was used in this study. Her age, height, weight, and cause of death were 88 years, 1,360 mm, 38 kg, and pancreatic cancer, respectively.

The cadaver was frozen at −70°C. After a week, the frozen cadaver was placed into the embedding box and embedding agent (gelatin solution) was poured into the box. The embedding box was frozen again at −70°C (**Fig. 1A**) as described.[6]

On the cryomacrotome,[6] the embedding box including the cadaver was placed and sectioned serially at constant intervals: head (from crown to chin), 0.25 mm; trunk (from below chin to fingertip), 0.5 mm; and lower limb (from below fingertip to toe), 1 mm (**Fig. 1B**). After sectioning the embedding box, the box was moved to a designated location to photograph the sectioned surface. In the location, the sectioned surface of 434 mm (width) × 290 mm (height) size was photographed using Canon™ EOS 5DsR digital single-lens reflex was prepared (resolution, 8,688 × 5,792; color depth, 48-bit color) with the two strobes to make a sectioned image of 0.05 mm-sized pixel (**Fig. 1C**). To prevent color loss, images were saved in a tagged image file format (TIFF). Similarly, sectioned images from head to toe were created (**Fig. 2**) as described.[6,11] Among the sectioned images of whole body, images of abdominal region were selected to identify lymph node stations and nearby structures for this study.

https://doi.org/10.3346/jkms.2023.38.e392

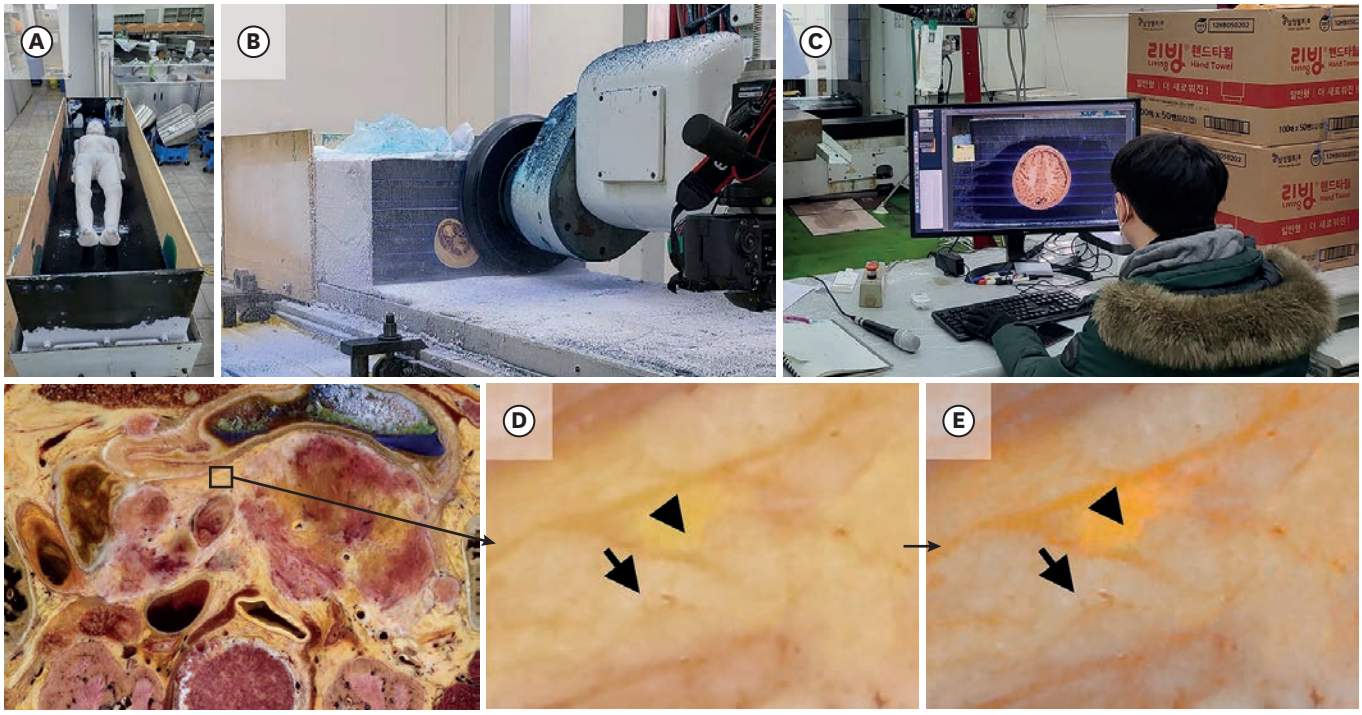

Fig. 1. Making processes of the sectioned images. (**A**) A cadaver is fixed by gelatin embedding agent in the embedding box. (**B**) Embedding box is milled by milling disc to make sectioned surface. (**C**) The sectioned surface is photographed and checked by anatomist to make sectioned image. Abdominal region in sectioned images of (**D**) original color and (**E**) a refined color after adjusting color purity in the image by Vibrance and Brightness/Contrast tools in Adobe Photoshop (Arrow = adipose tissue, Arrow head = parenchymal tissue of pancreas).

Fig. 2. Specimen sectioned images from head to toe of female whole body.

https://doi.org/10.3346/jkms.2023.38.e392

We needed to accurately separate the structures of similar colors in the sectioned images for accurate segmentation because the color of the pancreatic parenchymal tissue was similar to that of the adipose tissue around the pancreas. To convert the color of the sectioned images into as many different colors as possible, the color purity of the sectioned image was adjusted using the Vibrance tool and Brightness/Contrast tool in Adobe Photoshop 2022 (Adobe Systems, Inc., San Jose, CA, USA) (**Fig. 1D and E**).

The sectioned images were converted from TIFF to digital imaging and communication in medicine (DICOM) format after increasing the pixel size of the images from 0.05 to 1.0 mm. The DICOM files were reconstructed by volume modeling using dcm2niix in MRIcroGL 2018 (www.mccauslandcen-ter.sc.edu)[22] to create an abdominal volume model. In the volume model of MRIcroGL, the horizontal, coronal, and sagittal sectioned images were observed simultaneously to check the shape, position, and location of abdomen structures in the horizontal, coronal, and sagittal sectioned images (**Figs. 3** and **4**).

Based on the anatomy textbook[23] and atlas of lymph node anatomy,[21] the boundaries of 34 structures including 21 lymph nodes in the sectioned images of the abdominal region were

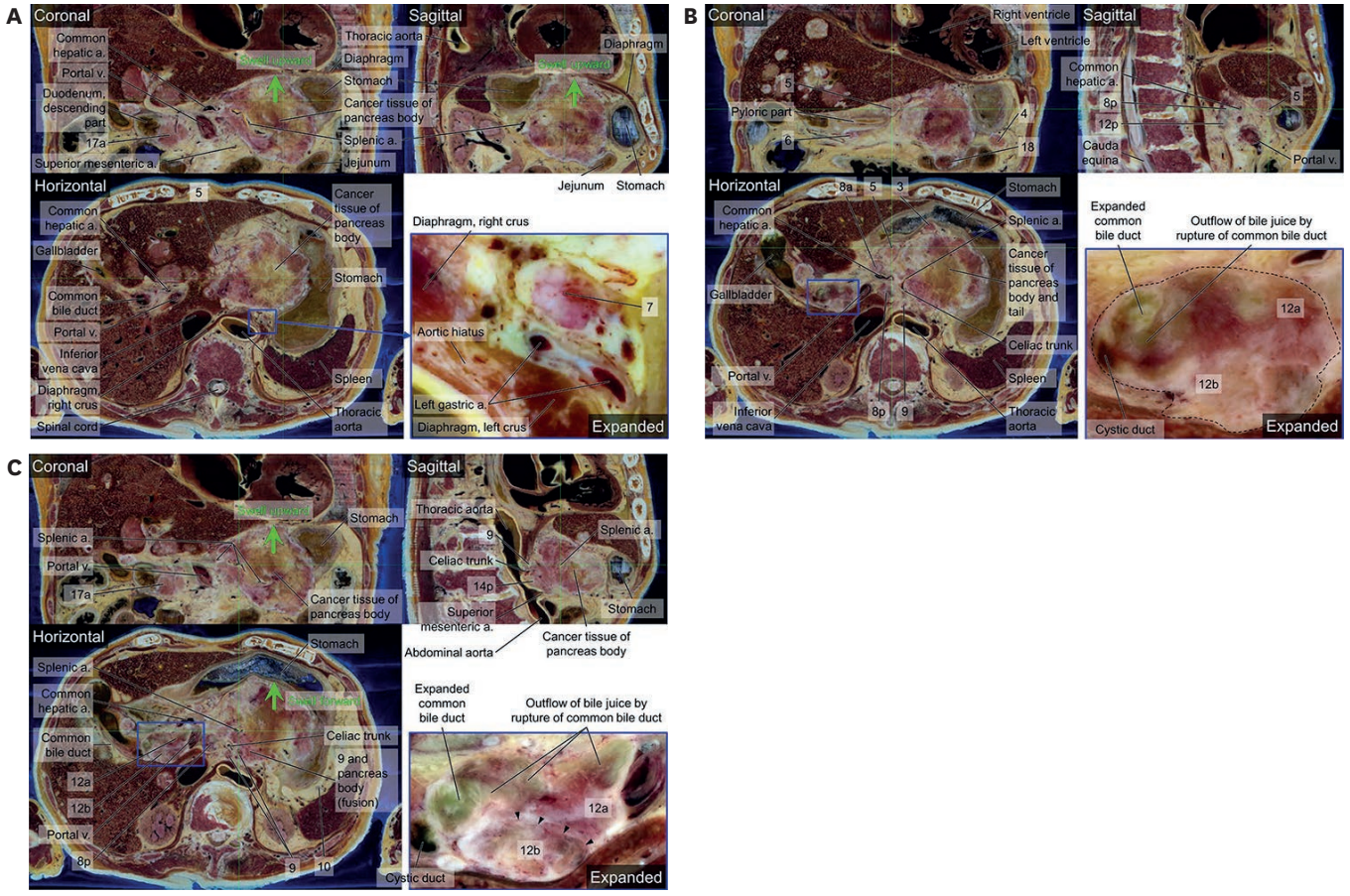

Fig. 3. Horizontal, coronal, and sagittal sectioned images from abdomen volume model on the MRIcroGL. Only horizontal images are aligned from top (**A**) to bottom (**C**) of the pancreas. (**A**) Both S-5 and S-7 are isolated from cancer tissue of pancreas. A part of cancer tissue of body of pancreas is touched in diaphragm, not stomach (Green arrow). Common bile duct is expanded. (**B**) S-3, S-5, S-6, S-8a, S-8p, and S-18 are separated whereas S-4, S-9, 12a, and 12b are fused with neighboring structures. There is serious cancer tissue in body of pancreas. (**C**) S-8p is isolated whereas S-9, S-12a, S-12b, S-14p, and S-17a are fused with cancer tissue of pancreas. S-12a and S-12b are fused together, but they can be divided (Arrow head). The stomach is squashed, due to swelling of the pancreas (Green arrow).'S-' is omitted in from S-1 to S-18.
a. = artery, v. = vein.

https://doi.org/10.3346/jkms.2023.38.e392

Table 1. Thirty-four segmented structures to create 3D models of the pancreas region

System	Structures
Digestive	Esophagus, Stomach, Intestine (small and large intestine), Liver, Gallbladder, Common hepatic duct, Cystic duct, Common bile duct, Pancreas
Urinary	Kidneys
Vascular	Artery (thoracic aorta, abdominal aorta, celiac trunk, left gastric artery, common hepatic artery, gastroduodenal artery, proper hepatic artery, right hepatic artery, left hepatic artery, cystic artery, splenic artery, superior mesenteric artery, inferior pancreaticoduodenal artery, inferior mesenteric artery, renal artery), Vein (inferior vena cava, renal vein, portal vein, superior mesenteric vein)
Lymphatic	Spleen, 21 lymph nodes (see **Table 2**)

3D = three-dimensional.

outlined using the Lasso tool and filled with specific colors using the Fill tool of Photoshop[24] to create segmented images of the bitmap (BMP) format (**Tables 1** and **2**).

In Mimics 10.01 (Materialise, Leuven, Belgium), the segmented images were reconstructed into 3D surface models using the Threshold and 3D objects - New function. Surface models of the segmented structures were saved in stereolithography (STL) format. In Deep exploration 6.3 (SAP America, Inc., Newton Square, PA, USA), entire surface models were assembled

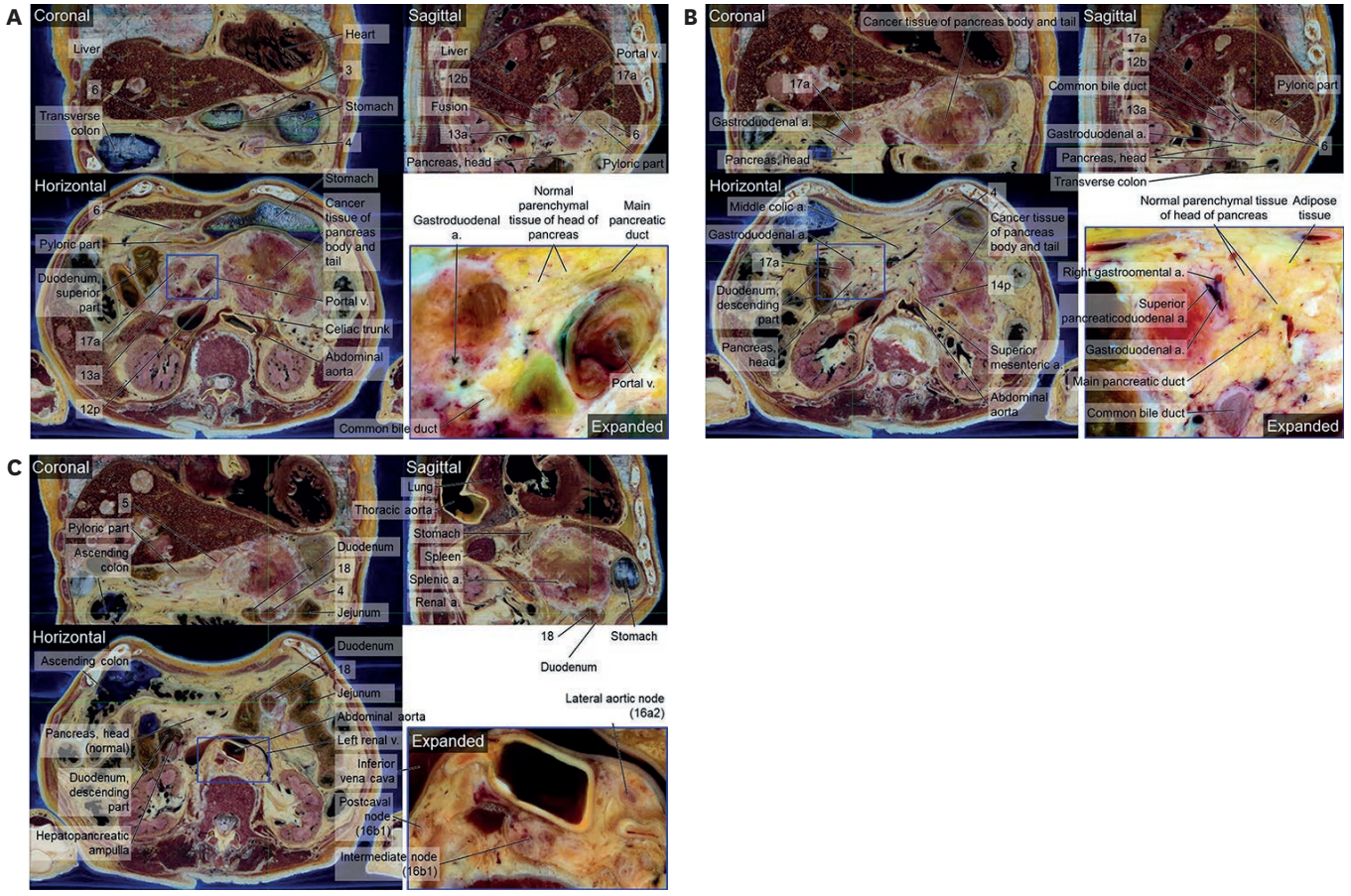

Fig. 4. Horizontal, coronal, and sagittal sectioned images from abdomen volume model on the MRIcroGL. Only horizontal images are aligned from top (**A**) to bottom (**C**) of the pancreas. (**A**) S-3 and S-6 are isolated respectively whereas 4, 12b, 12p, 13a, and 17a are fused with one another or pancreas. In the inferior portion of head of pancreas, normal parenchymal tissue is observed. (**B**) In the inferior portion of head of pancreas, normal tissue is larger than abnormal tissue. S-6 is isolated and S-4, S-12b, S-13a, S-14p, and S-17a are fused. (**C**) S-4, S-5, and 18 are observed. Duodenum is pressed by S-18. In the case of S-16a2 and 16b1, there were left lumbar nodes (Lateral aortic nodes), intermediate lumbar nodes, right lumbar nodes (postcaval nodes) as anatomical terminology. 'S-' is omitted in from S-1 to S-18.
a. = artery, v. = vein.

https://doi.org/10.3346/jkms.2023.38.e392

into a portable document format (PDF) file. The entire procedures of segmentation and 3D reconstruction were elucidated in the previous studies.[4,19,21]

On the sectioned images in the horizontal, coronal, and sagittal planes and the surface models, the pancreas with cancer tissue was distinguished, and lymph node metastases were analyzed in 28 stations (**Table 2**, **Figs. 3-5**).

Table 2. Classification of 28 lymphatic nodes around the pancreas in the sectioned images based on the Japanese Pancreas Society[21] and Terminologia Anatomica[25]

Clinical terms of the Japanese Pancreas Society		Anatomical terms of Terminologia Anatomica	size	Situation
Station	Definition			
S-1	Right cardial lymph nodes	Left gastric node (nodes around cardia)	Enlarged	Solitary
S-2	Left cardial lymph nodes		Enlarged	Solitary
S-3	Lymph nodes along the lesser curvature of the stomach	Right gastric nodes	Enlarged	Solitary
S-4	Lymph nodes along the greater curvature of the stomach	Right gastro-omental nodes Left gastro-omental nodes	Enlarged	Fused to cancer tissue in the pancreas body
S-5	Suprapyloric lymph nodes	Suprapyloric node	Enlarged	Solitary
S-6	Infrapyloric lymph nodes	Subpyloric nodes or Retropyloric nodes	Enlarged	Solitary
S-7	Lymph nodes along the left gastric artery	Left gastric node	Normal	Solitary
S-8a	Lymph nodes in the anterosuperior group along the common hepatic artery	Hepatic nodes	Enlarged	Solitary
S-8p	Lymph nodes in the posterior group along the common hepatic artery	Hepatic nodes	Enlarged	Solitary
S-9	Lymph nodes around the celiac artery	Celiac node	Enlarged	Fused to cancer tissue of the pancreas body and S-14p
S-10	Lymph nodes at the splenic hilum	Pancreaticosplenic node	Normal	Solitary
S-11p	Lymph nodes along the proximal splenic artery	Pancreaticosplenic node = splenic node	Fused	Fused to cancer tissue in the pancreas body
S-11d	Lymph nodes along the distal splenic artery	Pancreaticosplenic node = splenic node	Fused	Fused to cancer tissue in the pancreas body
S-12a	Lymph nodes along the proper hepatic artery in the hepatoduodenal ligament	Hepatic node	Enlarged	Fused to S-12b behind S-12a
S-12p	Lymph nodes along the portal vein in the hepatoduodenal ligament	Hepatic node	Enlarged	Fused to 8p below S-12p
S-12b	Lymph nodes along the bile duct in the hepatoduodenal ligament	Hepatic node	Enlarged	Fused to the common bile duct and S-13a
S-13a	Lymph nodes on the posterior aspect of the superior portion of the head of the pancreas	Pancreaticoduodenal lymph node (superior nodes)	Enlarged	Fused to S-12b and to the pancreas head
S-13b	Lymph nodes on the posterior aspect of the inferior portion of the head of the pancreas	Pancreaticoduodenal lymph node (inferior nodes)	Absence	
S-14p	Lymph nodes on the proximal superior mesenteric artery	Superior mesenteric lymph node	Enlarged	Fused to the pancreas body
S-14d	Lymph nodes along the distal superior mesenteric artery	Superior mesenteric lymph node	Absence	
S-15	Lymph nodes along the middle colic artery	Middle colic nodes	Absence	
S-16a1	Lymph nodes around the aortic hiatus of the diaphragm	Phrenic nodes	Absence	
S-16a2	Lymph nodes around the abdominal aorta (from the superior margin of the celiac trunk to the inferior margin of left renal vein)	Left lumbar nodes (lateral aortic nodes, postaortic nodes), intermediate lumbar nodes	Enlarged	Solitary
S-16b1	Lymph nodes around the abdominal aorta (from the inferior margin of the left renal vein to the superior margin of the inferior mesenteric artery)	Left lumbar nodes (postaortic nodes), intermediate lumbar nodes, right lumbar nodes (lateral aortic nodes, postaortic nodes, postcaval nodes)	Enlarged	Solitary
S-16b2	Lymph nodes around the abdominal aorta (from the superior margin of the inferior mesenteric artery to the aortic bifurcation)	Left lumbar nodes (postaortic nodes)	Enlarged	Solitary
S-17a	Lymph nodes on the anterior surface of the superior portion of the head of the pancreas	Pancreaticoduodenal lymph node (superior nodes)	Enlarged	Fused to cancer tissue in the pancreas head
S-17b	Lymph nodes on the anterior surface of the inferior portion of the head of the pancreas	Pancreaticoduodenal lymph node (inferior nodes)	Absence	
S-18	Lymph nodes along the inferior margin of the pancreas	Pancreatic nodes (inferior nodes)	Enlarged	Fused to the pancreas body

https://doi.org/10.3346/jkms.2023.38.e392

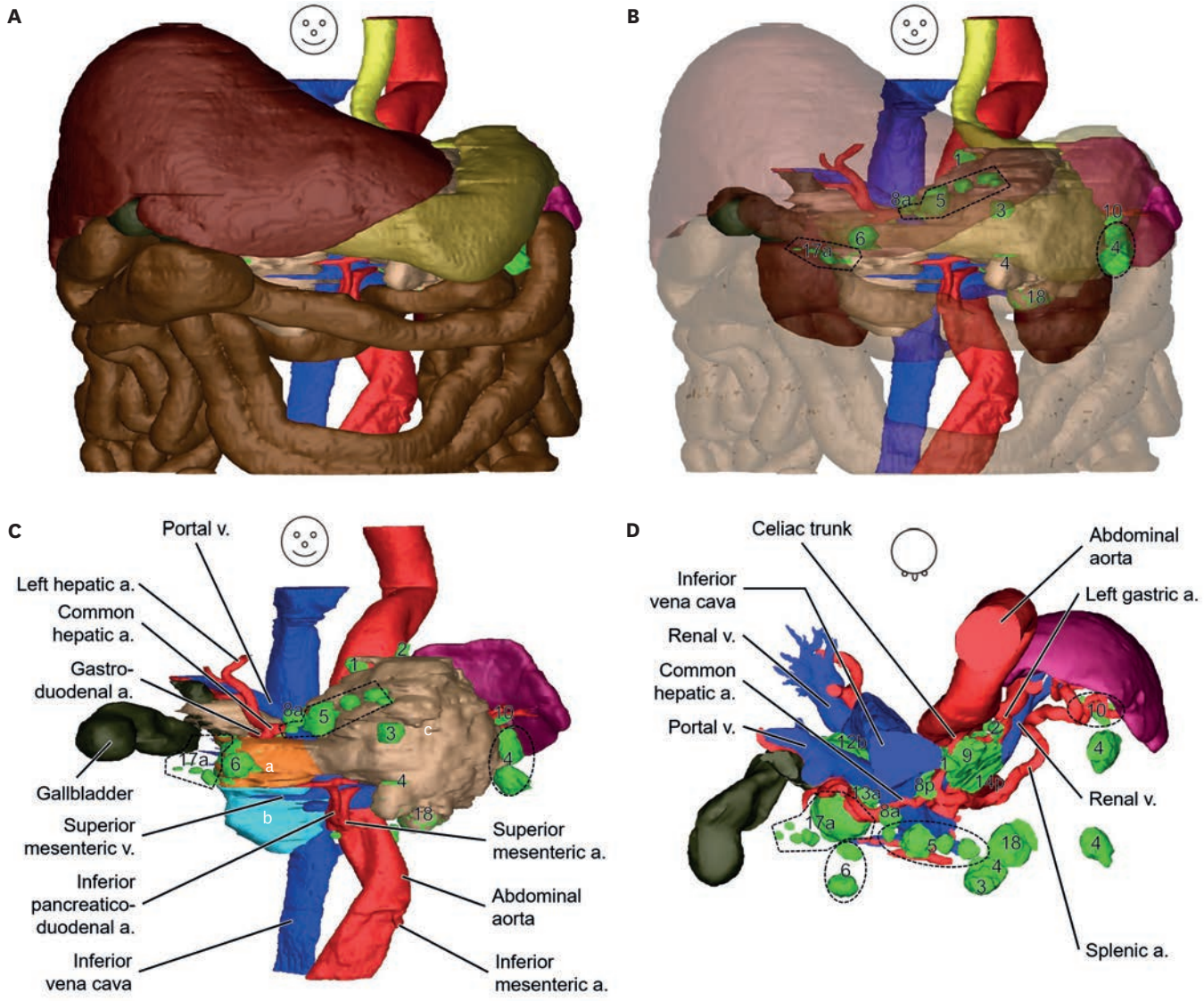

Fig. 5. Surface models of abdominal region including pancreatic cancer and its lymph node metastases. (**A**) Shape and location of structures of the abdominal region are observed opaquely. (**B**) In anterior view of translucent liver, stomach, small intestine, and large intestine, lymph node stations can be observed. (**C**) In the anterior view of structures except liver, stomach, small intestine, large intestine, and kidney, lymph node stations around the pancreas are identified in green. (**D**) In the superior view, lymph node stations around branches of the celiac trunk are identified.
a. = artery, v. = vein.
[a]Superior and [b]Inferior portions of head of pancreas, [c]Body and tail of pancreas.

Ethics statement

After we received informed consent for research and publication from the bereaved family, we obtained permission for this study from the Institutional Review Board of Dongguk University School of Medicine (IRB, number DGU-IRB-20220032).

RESULT

For this study, 2,716 sectioned images of the entire body were produced at constant intervals (head, 0.25 mm; trunk, 0.5 mm; and lower limb, 1.0 mm) and small pixel size (0.05 mm) (**Fig. 2**)

https://doi.org/10.3346/jkms.2023.38.e392

from the female cadaver (**Fig. 1A**). To discriminate the structures exactly, the sectioned images were made in 48-bit color, which could express 281,474,976,710,656 colors in a pixel. Owing to these intervals, pixel size, and color depth, not only macro- and microstructures but also simple and complicated structures in the entire body could be identified in the sectioned images (**Figs. 2**-**4**). In this study, we analyzed pancreatic cancer and lymph node metastases in the sectioned images (**Figs. 3** and **4**) and surface models (**Fig. 5**) of the abdominal region as follows.

Pancreas and its ducts with cancer tissue

The head of the normal pancreas is surrounded by the duodenum and the superior mesenteric vessels behind the stomach.[23] In these sectioned images, the left, right, and inferior portions of the head were surrounded, similar to the normal pancreas. However, the anterior and posterior surfaces of the superior portion of the head were fused with lymph nodes, due to lymph node metastases (stations [S]-17a and S-13a) (**Figs. 3A**, **4A**, **5C** and **5D**, **Table 2**). Fortunately, the inferior portion of the head was normal (**Figs. 4C** and **5C**). We decided the borderline between the superior and inferior portions of the head, where the gastroduodenal artery divided the superior pancreaticoduodenal artery and the right gastroomental artery (**Figs. 4B** and **5C**).

The body and tail of the pancreas were surrounded by the superior mesenteric vessels (right side), splenic artery (superior side), and spleen (left side) behind the stomach.[23] In these sectioned images, the body was swollen above and below the splenic artery due to the pancreatic cancer. Hence, the stomach was pushed upward and forward by the swollen body (**Fig. 3C**), and part of the cancer tissue of pancreas touched the diaphragm (**Fig. 3A**). Commonly, the tail is attached to the spleen[23]; however, no part of this pancreas was attached to the spleen. All bodies and tails turned into cancer tissue (**Fig. 3**), whereas normal tissue existed in the inferior portion of the head of the pancreas (**Figs. 4C** and **5**).

The left and right common hepatic ducts and common bile duct were observed between the pancreas and liver; however, one part of the common bile duct was dilated to the point of bursting because the duct was fused to the lymph node metastasis (S-12, **Table 2**) in the hepatoduodenal ligament (**Fig. 3**).

In the pancreas, the main and accessory pancreatic ducts were compressed by the swollen body and tail owing to pancreatic cancer. Thus, the lumen of the ducts was very narrow (**Fig. 4B**); however, the hepatopancreatic ampulla, connected to the common bile duct and main pancreatic duct, was swollen (**Fig. 3C**) and opened to the second part of the duodenum.

Lymph node metastases around the pancreas

In the sectioned images, some lymph nodes were observed isolated, and some nodes were fused to the pancreatic cancer tissue or neighboring nodes. The nodes were considered metastasized because of the enlarged size or different colors of the tissue, unlike in normal tissue. Based on the Japan Pancreas Society Classification,[4,5,21] 28 stations of lymph nodes were described in the horizontal, coronal, and sagittal sectioned images as follows. Furthermore, following all stations were organized and compared using the anatomical terminology[25] in **Table 2**.

S-1 and S-2 were placed on the right and left sides of cardia of stomach (**Fig. 5C**); therefore, their anatomical terms were nodes around the cardia.

https://doi.org/10.3346/jkms.2023.38.e392

S-3 and S-4 were placed above (lesser curvature) and below (greater curvature) the stomach in the coronal plane (**Fig. 4A**) and 3D view (**Fig. 5B-D**). S-4 fused to the cancer tissue of the pancreatic body (**Fig. 4B**). In the lesser and greater curvatures of the stomach, the right gastric artery and right (left) gastroomental artery are present; therefore, the anatomical terms of these lymph nodes are the right gastric nodes and right (left) gastroomental nodes.

S-5 and S-6 nodes were placed above and below the pyloric part of the stomach in the coronal plane (**Figs. 3B** and **4A**), sagittal plane (**Fig. 4B**), and 3D view (**Fig. 5B**), respectively. Their positions are exactly above and below the pyloric part of the stomach; therefore, their anatomical terms are suprapyloric and infrapyloric lymph nodes.

S-7 node was noted in front of the left gastric artery (**Fig. 3A**); therefore, its anatomical term was left gastric node.

S-8a and S-8p nodes were placed in the anterior and posterior areas of the common hepatic artery in the horizontal plane (**Fig. 3B**) and 3D view (**Fig. 5C**). S-8p was located above S-12p (**Fig. 3B**).

S-9 was placed bilaterally to the celiac trunk. The right celiac node was separated, whereas the lateral area of the left celiac node was fused with the cancer tissue of the pancreatic body and its inferior area was fused with S-14p in sectional planes (**Figs. 3C**) and 3D view (**Fig. 5D**).

S-10 was small around the hilum of the spleen, similar to a normal lymph node (**Fig. 5D**); however, its dark color was not normal. Conversely, the splenic artery and vein were not of normal size in the hilum of the spleen because the cancer tissue was present in the pancreas (**Fig. 3C**).

S-11p and S-11d around the splenic artery were indistinguishable in the pancreas because cancer tissue covers the artery. Around the splenic artery, the lymph nodes appeared to be fused to cancer tissues in the pancreatic body and tail (**Fig. 3C**).

S-12a and S-12b were placed around the common hepatic artery and common bile duct in the hepatoduodenal ligament, respectively (**Fig. 5D**). However, between the liver and pancreatic head, both S-12a and S-12b were fused with the common bile duct except for the common hepatic artery and portal vein (**Fig. 3B and C**). Part of the lymph node boundaries could be separated (**Fig. 3C**). The inferior area of S-12b was also fused with S-13a (**Fig. 4A**).

S-13a was placed in the posterior area of the superior portion of the pancreatic head and fused with not only S-12b but also S-17a (**Figs. 4A** and **5D**). The posterior area of the inferior portion of the pancreatic head was normal; thus, S-13b could not be observed (**Figs. 4C** and **5C**).

S-14p was placed left to the proximal superior mesenteric artery (**Figs. 4B** and **5D**). S-14p fused sagittally below S-9 between the celiac trunk and the superior mesenteric artery (**Fig. 3C**) and horizontally with the cancer tissue of the pancreatic body in the anterolateral area of the superior mesenteric artery (**Fig. 4B**). In the inferior area of the pancreas, S-14p was separated from the pancreatic body. S-14d was invisible because of the cancer tissue in the pancreatic body.

S-15 was invisible around the middle colic artery. Normal tissue was observed around the artery in the horizontal plane (**Fig. 4B**).

https://doi.org/10.3346/jkms.2023.38.e392

S-16 around the abdominal aorta consisted of S-16a1, S-16a2, S-16b1, and S-16b2. S-16a1 around the aortic hiatus was very small or invisible; therefore, we concluded that no lymph node metastasized there. In the S-16a2 range, the left lumbar nodes (lateral aortic and postaortic nodes) and intermediate lumbar nodes were enlarged and visible near the left renal vein rather than the celiac trunk. In S-16b1, the left (postaortic), intermediate, and right lumbar nodes (lateral aortic, postaortic, and postcaval nodes) (**Fig. 4C**) were identified based on anatomical terminology.[25] In S-16b2, only the left lumbar nodes (postaortic nodes) were present.

S-17a was located on the anterior surface of the superior portion of the pancreatic head, and its entire tissue changed into cancer tissue. The posterior area of S-17a was fused with S-13a (**Figs. 4A** and **5D**). The inferior portion of S-17a was in contact with the normal pancreatic head tissue (**Figs. 4A**, **4B**, and **5D**). S-17b was invisible in the inferior portion of the pancreatic head.

S-18 was located in the inferior part of pancreatic body. Its enlarged cancer tissue invaded the duodenum and almost blocked the duodenal tract, although no other lesions were found in the duodenum (**Figs. 4C** and **5D**).

Lymphatic drainage from the pancreas to thoracic duct

In the normal pancreas, lymph nodes on the head of the pancreas drain to those around the superior mesenteric artery and the celiac trunk through the lymphatics around the hepatoduodenal ligaments. Lymph nodes on the body and tail of the pancreas drains to those on the splenic and superior mesenteric arteries and to the celiac trunk through lymphatics on the hepatoduodenal ligaments.[23] In summary, all lymph nodes in the pancreas flow to the lymph nodes in the superior mesenteric artery and celiac trunk through the lymphatics of the hepatoduodenal ligaments. Therefore, the S-9 (celiac node) and S-14p (superior mesenteric lymph node) were significantly large (**Figs. 3C** and **4B**), and S-8 and S-12 (hepatic nodes) fused or ruptured in the hepatoduodenal ligaments (**Fig. 3B and C**). As fusion and rupture of the lymph nodes occurred, the common bile duct appeared to rupture in the hepatoduodenal ligaments (**Fig. 3B and C**).

Abnormal structures, directly affected by pancreatic cancer

The stomach was not invaded by the pancreatic cancer tissue, although it was pushed upward and forward because of the pancreatic cancer (**Fig. 3C**). The duodenum was invaded by enlarged cancer tissue of S-18 at the inferior boundary of the pancreatic body (**Figs. 4C** and **5C**).

In the liver, several cancer masses and lymph node metastases were identified based on their abnormal colors and shapes. The cystic duct of the gallbladder expanded (**Fig. 3B and C**).

In the branches of the celiac trunk, the splenic artery was buried in the cancer tissue of the pancreatic body, making it difficult to ascertain the artery. The left and right gastro-omental arteries were invisible because the greater curvature of the stomach was pushed by the pancreatic cancer tissue (**Fig. 3C**).

DISCUSSION

The identification of lymph node stations relevant to pancreatic cancer in the sectioned images of this study is reliable. To identify structures in the sectioned images accurately, the color purity of the sectioned images was adjusted using the Vibrance tool and Brightness/Contrast

https://doi.org/10.3346/jkms.2023.38.e392

tool in Adobe Photoshop 2022 as the first step. In the color-adjusted sectioned images, the basis of identifying lymph node metastases and cancer tissue in the head, body, and tail of the pancreas were large, reddish, or yellowish, and out of the normal place. This information is reliable because it is visible to the naked eye and is undeniable, factual information.

In the cadaver of this study, pancreatic cancer occurred in the entire pancreas, even though up to two-thirds of pancreatic cancers are commonly located in the head of the pancreas.[23] Therefore, we demonstrated not only metastases on 28 lymph node stations and the entire pancreas with cancer, but also related structures by using shape, location, and color in the sectioned images (**Figs. 3** and **4**) and 3D view (**Fig. 5**). In the images, the pancreas was already a cancer mass in size and color, regardless of the observer. Furthermore, most lymph node metastases were confirmed because of their large size and reddish color (**Figs. 3** and **4**). A few lymph nodes, such as S-7, were normal in size but reddish in color (**Fig. 3A**); hence, we considered that metastasis occurred. In fact, the diagnosis of cancer and metastasis of a structure are determined by histological findings after biopsy; however, some cancers and lymph node metastases are directly diagnosed and removed by surgeons in the operating room without histological findings, because surgeons are convinced of the abnormal structures through size and color. Similar to the surgeons, we were sure that they were cancer and metastasized through their obviously different size, shape, and color compared to anatomically normal tissues of other previous series of sectioned images (**Figs. 3** and **4**).[3,4]

This study provides the horizontal, coronal, and sagittal sectioned images in volume models (**Figs. 3** and **4**) and surface models (**Fig. 5**) as well as lymph node station information (**Table 2**) of a patient with pancreatic cancer. According to the provided data, we classified two categories of severe metastatic sites in considering severity of lymph node metastases from pancreatic cancer.

The first site was located in the pancreas. The S-11 (splenic nodes) were completely merged into the cancer tissue in the body and tail of pancreas, which we could not locate the boundaries of the nodes (**Figs. 3C** and **5**). Around the head of pancreas, S-13 and S-17 (pancreaticoduodenal lymph nodes) were also merged into cancer tissue. We could only find a part of the outer boundaries of these nodes because the inner part of the nodes was fused to the pancreas (**Figs. 4** and **5**).

The second was around the hepatoduodenal ligament. S-12 (hepatic nodes) were placed in the hepatoduodenal ligament which contains lymphatics from the pancreas (downstream) to S-9 (celiac node) (upstream). As all serious lymph node metastases occurred in the ligament, S-12 was fused or crushed, and the common bile duct ruptured (**Fig. 3B and C**).

Sectioned images of vivid color are as clinically valuable as CT and MRI grayscale images. Both the color and resolution of the structures are the most important factors in the reading of structural shapes in an image. Recently, although the resolution of MRI of 7 Tesla or even better has increased dramatically,[26,27] the resolving power of MRI is still limited because of the gray color of MRI. In the sectioned images, the vivid color and real shape of not only lymph node metastases but also pancreatic cancer were displayed (**Figs. 3** and **4**). Therefore, the clinical value of sectioned images is that they can display lymph nodes and cancer more clearly than CT and MRI.

Also, sectioned images of the entire body are as clinically valuable as CT and MRI of a part of the body. In the human body, one structure is connected to other structures, whether near or far apart. Therefore, medical doctors, even dentists, must learn regarding the gross anatomy

https://doi.org/10.3346/jkms.2023.38.e392

of the entire human body. In case of CT and MRI, taking a consistent CT or MRI of the whole body is difficult because each part of the body has different scanning conditions and sequences. Therefore, examining the organic connections of each structure is difficult using CT and MRI. Unlike CT and MRI, the entire body can be displayed in detail in the sectioned images (**Fig. 2**). The clinical value of sectioned images is that they can clearly display changes throughout the entire body caused by cancer and lymph nodes, which is not possible with CT or MRI.

This study suggests the better nomenclature of lymph node stations. In the Japanese Pancreas Society,[21] lymph nodes around the pancreas were named only by their serial numbers (**Table 2**). A serial number has the advantage of being able to differentiate structures in detail but has the disadvantage of not being able to determine the location of the structures. In the anatomical terminology,[25] lymph nodes around the pancreas were named based on location and direction (**Table 2**) as the general nomenclature of anatomical terminology. Anatomical terms have the advantage of being able to determine the location and shape of structures; however, they have the disadvantage of not being able to differentiate adjacent structures. For example, anatomical terms S-8 and S-12 were the only hepatic nodes (**Table 2**). The Japanese Pancreas Society and its anatomical terminology have both advantages and disadvantages. Therefore, we suggest the use of anatomical terminology for students and the Japanese Pancreas Society serial numbers for medical doctors.

Before this study, regarding pancreatic cancer and lymph node metastases, medical students and doctors only read textbooks with schematic figures and had no choice but to observe the severely deformed structures of a patient in a surgical operating room or cadavers. In this study, we presented the sectioned images in which the real color and shape of not only the pancreatic cancer and its lymph nodes but also neighboring normal structures could be observed in the entire body (**Figs. 3-5**). Consequently, in this study, we achieved the aim of identifying the shape, location, and positional relationship of pancreatic cancer with lymph node metastasis based on the sectioned images.

On the other hand, we presented the first sectioned images of the female body with a normal pancreas in 2010.[7] We will distribute results of this study including sectioned images of abnormal (this study) and normal pancreas (2010) on the author's homepage (neuroanatomy.kr) to help students, researchers, and medical doctors who need to study clinical anatomy of the pancreas.

ACKNOWLEDGMENTS

This study was a part of the Visible Korean Project of Professor Min Suk Chung (Ajou University School of Medicine). The authors of this study are collaborating with Professor Chung, and facilities for this study were supported by Ajou University.

REFERENCES

1. Kim KS, Kwon J, Kim K, Chie EK. Impact of resection margin distance on survival of pancreatic cancer: a systematic review and meta-analysis. *Cancer Res Treat* 2017;49(3):824-33.
PUBMED | CROSSREF

2. Rhee H, Park MS. The role of imaging in current treatment strategies for pancreatic adenocarcinoma. *Korean J Radiol* 2021;22(1):23-40.
PUBMED | CROSSREF
3. Zhang J, Zhang L, Li C, Yang C, Li L, Song S, et al. LOX-1 is a poor prognostic indicator and induces epithelial-mesenchymal transition and metastasis in pancreatic cancer patients. *Cell Oncol (Dordr)* 2018;41(1):73-84.
PUBMED | CROSSREF
4. Isaji S, Murata Y, Kishiwada M. New Japanese Classification of Pancreatic Cancer. In: Neoptolemos JP, Urrutia R, Abbruzzese JL, Büchler MW, editors. *Pancreatic Cancer*. New York, NY, USA: Springer New York; 2018, 1021-37.
5. Sobin LH, Gospodarowicz MK, Wittekind C. *TNM Classification of Malignant Tumours*. Hoboken, NJ, USA: John Wiley & Sons; 2011.
6. Park JS, Chung MS, Hwang SB, Lee YS, Har DH, Park HS. Visible Korean human: improved serially sectioned images of the entire body. *IEEE Trans Med Imaging* 2005;24(3):352-60.
PUBMED | CROSSREF
7. Park HS, Choi DH, Park JS. Improved sectioned images and surface models of the whole female body. *Int J Morphol* 2015;33(4):1323-32.
CROSSREF
8. Chung BS, Han M, Har D, Park JS. Advanced sectioned images of a cadaver head with voxel size of 0.04 mm. *J Korean Med Sci* 2019;34(34):e218.
PUBMED | CROSSREF
9. Shin DS, Jang HG, Hwang SB, Har DH, Moon YL, Chung MS. Two-dimensional sectioned images and three-dimensional surface models for learning the anatomy of the female pelvis. *Anat Sci Educ* 2013;6(5):316-23.
PUBMED | CROSSREF
10. Park JS, Chung MS, Shin DS, Har DH, Cho ZH, Kim YB, et al. Sectioned images of the cadaver head including the brain and correspondences with ultrahigh field 7.0 T MRIs. *Proc IEEE Inst Electr Electron Eng* 2009;97(12):1988-96.
CROSSREF
11. You Y, Kim CY, Kim SK, Chung BS, Har D, Choi J, et al. Advanced-sectioned images obtained by microsectioning of the entire male body. *Clin Anat* 2022;35(1):79-86.
PUBMED | CROSSREF
12. You Y, Park JS. A novel human brainstem map based on true-color sectioned images. *J Korean Med Sci* 2023;38(10):e76.
PUBMED | CROSSREF
13. Kim SK, Hur MS, Park JS. Real color sectioned images and correspondence with ultrasound images of the palmar wrist. *Appl Sci* 2022;12(1):299.
CROSSREF
14. Park JS, Jung YW. Peeled images and sectioned images from real-color volume models of foot. *Surg Radiol Anat* 2021;43(1):37-43.
PUBMED | CROSSREF
15. Kim CY, Park JS, Chung BS. Real color model of a cadaver for deep brain stimulation of the subthalamic nucleus. *Appl Sci* 2021;11(11):4999.
CROSSREF
16. Chung BS, Park HS, Park JS, Hwang SB, Chung MS. Sectioned and segmented images of the male whole body, female whole body, male head, and female pelvis from the Visible Korean. *Anat Sci Int* 2021;96(1):168-73.
PUBMED | CROSSREF
17. Park JS. 2D browsing software and 3D PDF of canine ear based on real color sectioned images. *Int J Morphol* 2020;38(1):147-52.
CROSSREF
18. Kwon K, Park JS, Shin BS. Virtual anatomical and endoscopic exploration method of internal human body for training simulator. *J Korean Med Sci* 2020;35(12):e90.
PUBMED | CROSSREF
19. Park JS. *Cross-Sectional Atlas of the Human Head: With 0.1-mm Pixel Size Color Images*. Berlin, Germany: Springer; 2018.
20. Park JS, You Y. *Cross-Sectional Atlas of Human Brainstem: With 0.06-mm Pixel Size Color Images*. Singapore: Springer Nature Singapore; 2023.

21. Harisinghani MG. *Atlas of Lymph Node Anatomy*. 2nd ed. Cham, Switzerland: Springer Nature Switzerland AG; 2013, 59-88.
22. Chung BS, Park JS. Real-color volume models made from real-color sectioned images of Visible Korean. *J Korean Med Sci* 2019;34(10):e86.
PUBMED | CROSSREF
23. Moore KL, Dalley AF, Agur AM. *Clinically Oriented Anatomy*. 8th ed. Philadelphia, PA, USA: Wolters Kluwer; 2018, 488-91.
24. Park JS, Chung MS, Hwang SB, Lee YS, Har DH. Technical report on semiautomatic segmentation using the Adobe Photoshop. *J Digit Imaging* 2005;18(4):333-43.
PUBMED | CROSSREF
25. FCAT. *Terminologia Anatomica*. Book & CD-ROM edition ed. New York, NY, USA: Thieme Medical Publishers; 2002.
26. Ertürk MA, Raaijmakers AJ, Adriany G, Uğurbil K, Metzger GJ. A 16-channel combined loop-dipole transceiver array for 7 Tesla body MRI. *Magn Reson Med* 2017;77(2):884-94.
PUBMED | CROSSREF
27. Rahman N, Xu K, Budde MD, Brown A, Baron CA. A longitudinal microstructural MRI dataset in healthy C57Bl/6 mice at 9.4 Tesla. *Sci Data* 2023;10(1):94.
PUBMED | CROSSREF